1.D.2

DESCRIPTION OF THE Pt AND Os ISOTOPES IN THE INTERACTING BOSON MODEL

R. BIJKER, A. E. L. DIEPERINK and O. SCHOLTEN

Kernfysisch Versneller Instituut, Groningen, The Netherlands

and

R. SPANHOFF †

Laboratorium voor Algemene Natuurkunde, Groningen, The Netherlands

Abstract: Properties of the even-even Pt and Os isotopes are investigated in the framework of the inter-
acting boson approximation, including the neutron-proton degree of freedom. It is shown that the
transition between the gamma unstable region of the heavier Pt isotopes towards the more axially
symmetric deformed features of the lighter Os and Pt isotopes can be described very well by the
IBA hamiltonian; qualitatively the properties of the transitional region are reproduced by the smooth
change of one parameter, χ_v, which determines the character of the quadrupole-quadrupole inter-
action. Calculated excitation energies and electromagnetic properties are compared with experiment.

1. Introduction

There exists a great variety of approaches to nuclear collective motion. While
almost all of these have in common that the basic degrees of freedom are represented
by the (five) quadrupole collective variables, the various models differ greatly both
conceptually and in practical aspects. While some of the models are completely
phenomenological, like the method of collective potential energy surfaces of Greiner
and collaborators [1,2], other models do have a relation to a microscopic picture but
are very complicated, like the boson expansion approach as applied by Kishimoto
and Tamura [3,4], or the pairing-plus-quadrupole model of Kumar and Baranger [5,6].

Recently a new approach to describe nuclear collective properties has been
proposed, the interacting boson approximation (IBA) of Arima and Iachello [7,10].
In this model, which has the virtue of being simple, the collective properties are
described in terms of pairs of nucleons coupled to angular momentum $L = 0$ and
$L = 2$, which are treated as bosons. In the original formulation of the model (hereafter
IBA-1) the many-body states are classified according to the totally symmetric
irreducible representations $[N]$ of the group SU(6). Here N represents the total

† Present address: Rijkswaterstaat, Hooftskade 1, 2526 KA The Hague, The Netherlands.

number of active proton and neutron pairs with respect to a closed core. The most general two-body hamiltonian within the boson space is written in terms of the generators of the groups SU(6). It has been shown, that in three special cases this hamiltonian can be expressed in terms of generators of a subgroup of SU(6), namely the SU(5) group [7], SU(3) group [8] and the O(6) group [9,10]. These extreme cases, which permit the construction of analytic solutions of energy spectra and transition rates, correspond (for $N \to \infty$) to the anharmonic vibrator, the axially symmetric deformed rotor, and the γ-unstable nucleus, respectively, of the geometrical picture.

The transitional regions between these extreme cases can also be treated in a simple way by numerical diagonalization of the SU(6) hamiltonian. As an example the transitional region between the SU(5) and SU(3) limits (experimentally observed in the Sm isotopes) has been investigated in detail in ref. [12]; it appeared that in this transitional region the energy spectra could be described by the variation of only one parameter, ε, the d-boson energy. Similarly the Pt and Os isotopes have been investigated as an illustration of the O(6) $\to$ SU(3) transition in the framework of IBA-1 by Casten and Cizewski [13]. In this case it was found that although many of the characteristic features of the nuclei in this region which are observed experimentally can be reproduced by the SU(6) model [especially B(E2) selection rules and branching ratios] the energy levels in the O(6) region could not be fitted satisfactorily in the IBA-1 approach, not even in a perturbed O(6) scheme.

More recently a generalized version of the IBA model has been proposed [11,14] in which neutron and proton boson degrees of freedom are treated independently (IBA-2). The physical motivation for treating neutrons and proton separately is that the interaction between like bosons is expected to be quite different from the one between unlike bosons. In fact it is well known that the strong and attractive neutron-proton interaction is mostly responsible for the collective behaviour of nuclei, and that in its absence (as in semi-magic nuclei) little collectivity occurs. Therefore IBA-2 seems to have a more direct microscopic foundation. In IBA-2 the states can be classified according to the group structure SU(6) $\otimes$ SU(6). Although it is possible to construct also in this case analytic solutions for limiting cases, most realistic applications require numerical diagonalization of the hamiltonian.

It appears that many features of the limiting cases of IBA-1 mentioned above are obtained for special choices of the parameters of the more general hamiltonian of IBA-2.

It is the aim of the present investigation to study nuclei around mass number $A = 190$, in a phenomenological way in the framework of IBA-2. The description of the overall trend will be emphasized more than the attempt to fit each nucleus in detail. As a result it will be possible to correlate a large amount of data in terms of few parameters. In addition, the information obtained in this way on the behaviour of the interaction parameters as a function of neutron and proton number can serve as a test of microscopic theories [15]. [Actual calculations are being performed by Otsuka et al. with promising results [11].]

In the present study specifically the Pt and Os isotopes with mass number $A \geq 184$ will be considered. In sect. 2 the structure of the IBA hamiltonian will be discussed. In sect. 3 the calculated energy spectra and two-neutron separation energies are presented and compared with experiment; results on electromagnetic transition rates are given in sect. 4. Other observables (two-neutron transfer cross sections, monopole properties) are discussed in sect. 5. Concluding remarks and a comparison with the results of other approaches are presented in sect. 6.

2. The IBA-2 model

2.1. THE IBA-2 HAMILTONIAN

The two-body hamiltonian in the IBA-2 formalism is expressed as [11,16]

$$H = \varepsilon_\pi n_{d\pi} + \varepsilon_v n_{dv} + \kappa Q_\pi^{(2)} \cdot Q_v^{(2)} + V_{\pi\pi} + V_{vv} + H_M + H_R + H_C. \tag{2.1}$$

Here the first two terms represent the single-boson energies for protons (π) and neutrons (v), respectively: $\varepsilon_{\pi(v)}$ is the energy difference between $d_{\pi(v)}$ and $s_{\pi(v)}$ bosons, and $n_{d\pi(v)}$ is the number of proton (neutron) d-bosons. For simplicity we will assume $\varepsilon_\pi = \varepsilon_v = \varepsilon$ in this work. The third term represents the main part of the boson-boson interaction, namely the quadrupole-quadrupole interaction between neutron and proton bosons with strength κ. The quadrupole operator is expressed as $(\rho = \pi, v)$

$$Q_\rho^{(2)} = (d_\rho^\dagger s_\rho + s_\rho^\dagger \tilde{d}_\rho)^{(2)} + \chi_\rho (d_\rho^\dagger \tilde{d}_\rho)^{(2)}. \tag{2.2}$$

The significance of the parameter χ_ρ which determines the structure of the quadrupole operator, will be discussed below. The terms $V_{\pi\pi} + V_{vv}$ represent d-boson conserving residual neutron-neutron and proton-proton interactions:

$$V_{\rho\rho} = \tfrac{1}{2} \sum_{\lambda = 0, 2, 4} C_{\lambda\rho} (d_\rho^\dagger d_\rho^\dagger)^{(\lambda)} \cdot (\tilde{d}_\rho \tilde{d}_\rho)^{(\lambda)}, \qquad \rho = \pi, v. \tag{2.3}$$

Such an interaction was found to be especially important near closed shell nuclei; in the vibrational limit it gives rise to a splitting of the SU(5) two-phonon triplet $(d^\dagger d^\dagger)^{(L)}|0\rangle$, $L = 0, 2, 4$. It can be argued [16] that the $V_{\pi\pi}(V_{vv})$ interaction is only important when one deals with a large number of active protons (neutrons) and a small number of active neutrons (protons).

The term H_M is given by

$$H_M = \xi_2 [(d_\pi^\dagger s_v^\dagger - s_\pi^\dagger d_v^\dagger)^{(2)} \cdot (s_v \tilde{d}_\pi - s_\pi \tilde{d}_v)^{(2)}] + \sum_{\lambda = 1, 3} \xi_\lambda (d_\pi^\dagger d_v^\dagger)^{(\lambda)} \cdot (\tilde{d}_\pi \tilde{d}_v)^{(\lambda)}, \tag{2.4}$$

and will be referred to as the majorana term for the following reason. In IBA-2, in addition to basis states that belong to the totally symmetric representation $[N]$ of SU(6), also states with an antisymmetric character occur corresponding to other representations of SU(6): $[N-1, 1]$, $[N-2, 2]$, ... It can be shown that the residual

boson-boson interaction has the property that the lowest eigenstates predominantly belong to the totally symmetric representation and therefore have a large overlap with the eigenstates obtained with IBA-1. We note that realistic hamiltonians like (2.1), in which the quadrupole-quadrupole interaction between the like and unlike bosons is different, in general will give rise to some mixing between the various SU(6) multiplets. The majorana operator has the property of shifting the various multiplets and can therefore conveniently be used to adjust the excitation energies of states with lower symmetry character. In the special case $\xi_1 = \xi_2 = \xi_3$ all states in a given multiplet are shifted by the same amount. The interaction proportional to ξ_1 and ξ_3 will affect mainly the low-lying $L^\pi = 1^+$ and 3^+ states in the $[N-1, 1]$ multiplet, respectively.

The term H_R represents additional interaction terms between the bosons, which on the basis of microscopic considerations are thought to be less important. For completeness they are given below:

$$H_R = \sum_{\lambda=0,2,4} G_\lambda (d_\pi^\dagger d_\nu^\dagger)^{(\lambda)} (\tilde{d}_\pi \tilde{d}_\nu)^{(\lambda)} + \sum_{\rho=\pi,\nu} \left[W_{2\rho} (d_\rho^\dagger d_\rho^\dagger)^{(2)} \cdot (\tilde{d}_\rho s_\rho)^{(2)} \right.$$

$$\left. + W_{0\rho} (d_\rho^\dagger d_\rho^\dagger)^{(0)} (s_\rho s_\rho) \right] + \text{h.c.} \tag{2.5}$$

Finally H_C contains interactions that affect binding energies but not excitation energies [12])

$$H_C = \sum_{\rho=\pi,\nu} (A_\rho N_\rho + \tfrac{1}{2} B_\rho N_\rho (N_\rho - 1)) + A_{\pi\nu} N_\pi N_\nu + C. \tag{2.6}$$

2.2. THE LIMITING CASES

It can be shown that for special choices of the parameters in eq. (2.1) solutions are obtained which are similar to the limiting cases constructed in IBA-1.

(a) "*The SU*(3) *limit.*" In the SU(3) limit of IBA-1 [ref. [8])] the hamiltonian is expressed in terms of the Casimir operators of the group chain SU(3) $\supset$ O(3). The energy eigenvalues are given by

$$E([N](\lambda, \mu)KLM) = \alpha L(L+1) + \beta(\lambda^2 + \mu^2 + \lambda\mu + 3(\lambda + \mu)), \tag{2.7}$$

where the SU(3) labels (λ, μ) take on the values $(\lambda, \mu) = (2N, 0)$ for the ground-state band and $(\lambda, \mu) = (2N - 4, 2)$ for the β- and γ-band. In IBA-2 the SU(3) features of axially symmetric deformed rotor are obtained by taking only the $\kappa Q_\pi^{(2)} \cdot Q_\nu^{(2)}$ interaction in (2.1) and neglecting all other interaction terms. This can be seen by rewriting

$$\kappa Q_\pi^{(2)} \cdot Q_\nu^{(2)} = \tfrac{1}{4}\kappa \{ (Q_\pi^{(2)} + Q_\nu^{(2)}) + (Q_\pi^{(2)} - Q_\nu^{(2)}) \} \cdot \{ (Q_\pi^{(2)} + Q_\nu^{(2)}) - (Q_\pi^{(2)} - Q_\nu^{(2)}) \}. \tag{2.7}$$

Since the low-lying eigenstates ψ_i predominantly belong to the symmetric representation of SU(6), the norm of the state $(Q_\pi^{(2)} - Q_\nu^{(2)})|\psi_i\rangle$ is small. Therefore the interaction

(2.7) can effectively be replaced by $H = \frac{1}{4}\kappa(Q_\pi^{(2)}+Q_\nu^{(2)}) \cdot (Q_\pi^{(2)}+Q_\nu^{(2)})$, which for $\chi_\nu = \chi_\pi = \pm\frac{1}{2}\sqrt{7}$ is a special case of the SU(3) hamiltonian of IBA-1 [ref. [8]].

(b) *"The O(6) limit."* In the O(6) limit the IBA-1 hamiltonian is expressed [9, 10] in terms of the Casimir operators of the group chain O(6) $\supset$ O(5) $\supset$ O(3). The eigenvalues can be written as

$$E([N], \sigma\tau\nu_\Delta LM) = \frac{1}{4}A(N-\sigma)(N+\sigma+4)+\frac{1}{6}B\tau(\tau+3)+CL(L+1), \qquad (2.8)$$

where the quantum numbers σ and τ (seniority) characterize the totally symmetric representations of the groups O(6) and O(5), respectively; they take on the values: $\sigma = N, N-2 \ldots; \tau = \sigma, \sigma-1, \ldots, 0$. For example, the ground-state band has $\sigma = N, L = 2\tau$, the 2_2^+ state $\sigma = N, \tau = 2$, and the 0_2^+ and 0_3^+ states have $\sigma = N, \tau = 3$ and $\sigma = N-2, \tau = 0$. Strictly speaking, in order to obtain the O(6) limit of the hamiltonian (2.1) the complete elimination of the one d-boson changing terms, i.e. $\chi_\nu = \chi_\pi = 0$, is required. It turns out, however, that the less stringent condition $\chi_\pi \approx -\chi_\nu$ also leads to spectra that have many of the O(6) features and in addition avoids some of the predictions of the pure O(6) limit, which do not agree with experiment, such as vanishing quadrupole moments. The choice $\chi_\pi = -\chi_\nu$ results in the elimination of the one-boson changing term in the interaction between symmetric states, and therefore these states can be characterized by the boson seniority quantum number τ of the O(6) limit [10]. In order to see things in more detail it is convenient to rewrite the quadrupole-quadrupole interaction as

$$Q_\pi^{(2)} \cdot Q_\nu^{(2)} = [(d_\nu^\dagger \tilde{d}_\pi)^{(0)}s_\pi^\dagger s_\nu+(d_\pi^\dagger \tilde{d}_\nu)^{(0)}s_\nu^\dagger s_\pi]+ \sum_{\rho\neq\rho'} \chi_{\rho'}(d_\rho^\dagger \tilde{d}_{\rho'})^{(2)} \cdot (d_\rho^\dagger s_\rho + s_\rho^\dagger \tilde{d}_\rho)^{(2)}$$

$$+ [(d_\pi^\dagger d_\nu^\dagger)^{(0)}s_\pi s_\nu+(\tilde{d}_\pi \tilde{d}_\nu)^{(0)}s_\pi^\dagger s_\nu^\dagger]+\chi_\pi\chi_\nu(d_\pi^\dagger \tilde{d}_\pi)^{(2)} \cdot (d_\nu^\dagger \tilde{d}_\nu)^{(2)}. \qquad (2.9)$$

The first term in eq. (2.9) gives rise to an effective contribution to ε; the second term is expected to give a small contribution when acting on states with maximum symmetry in case of $\chi_\pi \approx -\chi_\nu$. The third term can be regarded as the two d-boson changing parts of the O(6) pairing operator: $P_6 = \frac{1}{2}(d^\dagger \cdot d^\dagger - s^\dagger s^\dagger)(\tilde{d} \cdot \tilde{d} - ss)$. The last term in eq. (2.9) contains apart from a d-boson pairing term also O(6) symmetry breaking terms.

3. Energy spectra and binding energies

The hamiltonian (2.1) was diagonalized in a complete set of spherical basis states $[(d_\pi^\dagger)^{n_{d\pi}}(L_\pi\phi_\pi)(s_\pi^\dagger)^{N_\pi-n_{d\pi}}(d_\nu^\dagger)^{n_{d\nu}}(L_\nu\phi_\nu)(s^\dagger)^{N_\pi-n_{d\nu}}]^L|0\rangle$, where the labels ϕ_ν, ϕ_π are used to specify the states completely. The values of the proton (neutron) boson numbers $N_\pi(N_\nu)$ are determined by half the number of proton (neutron) holes with respect to the closed shells $Z = 82, N = 126$; i.e. $N_\pi = 2$ (3) for the Pt (Os) isotopes, and N_ν takes on the values 4 (^{196}Pt, ^{194}Os) to 9 (^{186}Pt, ^{184}Os).

3.1. CHOICE OF PARAMETERS

Since the hamiltonian contains many parameters it is unpractical and not very meaningful to vary all parameters freely. Instead it is convenient to use the behaviour of the parameters predicted by a microscopic point of view as a zeroth-order approximation. In a simple shell-model picture based upon degenerate single-nucleon levels [15]) the expected dependence of ε, κ, χ_ν and χ_π on neutron (N_ν) and proton (N_π) boson numbers can be expressed as:

$\varepsilon = $ constant,

$$\kappa = \kappa_\pi \kappa_\nu, \qquad \kappa_\rho = \sqrt{\frac{\Omega_\rho - N_\rho}{\Omega_\rho - 1}}\,\kappa_\rho^{(0)}, \qquad \chi_\rho = \frac{\Omega_\rho - 2N_\rho}{\sqrt{\Omega_\rho - N_\rho}}\,\chi_\rho^{(0)}, \qquad \rho = \pi, \nu. \quad (3.1)$$

Here $\kappa_\rho^{(0)}$ and $\chi_\rho^{(0)}$ are constants, and Ω_ρ is the pair degeneracy of the shell. We see that while κ_ρ has always the same sign, χ_ρ changes sign in the middle of the shell.

In realistic cases the estimates of eq. (3.1) are expected to be valid only approximately. In our approach we have imposed somewhat weaker constraints on the parameters: (i) it is assumed that within a series of isotopes (isotones) χ_π (χ_ν) does not vary at all; (ii) the parameters ε, κ and χ_ν are assumed to be smooth functions of N_ν.

Concerning the sign of χ_ν and χ_π a complication arises. From very simple microscopic considerations it follows [17]) that the χ's [which also determine to a large extent the sign of the quadrupole moment of the 2_1^+ state (see below)] are negative in the region where the valence shell is less than half filled (particle-bosons) and positive in the region where the valence shell is more than half filled (hole-bosons). Quantitatively, such a behaviour was confirmed in other phenomenological calculations with IBA-2. For example, in a study of the Ba isotopes with $72 < N < 80$ a good fit to the energy levels was obtained with $\chi_\nu \approx 0.90$ [ref. [16]]. Since in the naive shell-model picture in the Pt region both neutrons and protons are hole-like and therefore both χ's would be positive, there would be no way to obtain an O(6) type spectrum, which requires opposite signs of χ_ν and χ_π. This indicates that the situation is not so simple and that more complicated effects play a role, such as a possible non-closedness of the $Z = 82$ or the $N = 126$ core. Although the hamiltonian is invariant under a simultaneous change in sign of both χ_π and χ_ν and thus equally good fits to energy spectra can be obtained for both combinations $\chi_\nu > 0$, $\chi_\pi < 0$ and $\chi_\nu < 0$, $\chi_\pi > 0$ there is a preference for the choice $\chi_\nu > 0$, $\chi_\pi < 0$. Namely, only with this choice the observed sign of the mass quadrupole moment of the 2_1^+ state in ^{194,196}Pt can be reproduced (see sect. 4). In addition in this case the values of the parameters that are needed to describe the lighter Os isotopes which have a prolate rotor character $(\chi_\nu, \chi_\pi < 0)$ are smoothly connected to those of the Pt isotopes.

The remaining parameters play a less important role and are used mainly to improve the fit with experiment. In this paper only $C_{0\nu}$ and $C_{2\nu}$, representing part

TABLE 1

Parameters used in the IBA hamiltonian (in MeV)

Nucleus	ε	κ	χ_v	χ_π	C_{0v}	C_{2v}	C_{4v}	ξ_2	$\xi_1 = \xi_3$
^{196}Pt	0.58	−0.18	1.05	−0.80	0.60	0.02	0.00	0.04	−0.10
^{194}Pt	0.58	−0.18	0.95		0.55	0.04			
^{192}Pt	0.58	−0.18	0.80		0.45	0.00			
^{190}Pt	0.58	−0.18	0.45		0.00	−0.09			
^{188}Pt	0.58	−0.16	0.00		−0.25	−0.13			
^{186}Pt	0.62	−0.145	−0.50		−0.25	−0.16			
^{194}Os	0.45	−0.15	1.05	−1.30	0.60	0.02	0.00	0.04	−0.10
^{192}Os	0.45	−0.15	0.95		0.55	0.04			
^{190}Os	0.45	−0.15	0.80		0.45	0.00			
^{188}Os	0.45	−0.15	0.45		0.00	−0.09			
^{186}Os	0.45	−0.14	0.00		−0.25	−0.13			
^{184}Os	0.50	−0.135	−0.50		−0.25	−0.16			

of the d-boson conserving interaction between neutron bosons, were used as free parameters independent of N_π. Finally, the values of ξ_2 and $\xi_1 = \xi_3$ were kept constant. The parameters used for the various nuclei are shown in table 1 and the calculated energy spectra compared with experiment in figs. 1 and 2.

It is seen that parameters are constant or vary smoothly: within a series of isotopes χ_π does not vary, the variation in ε is very small and there is a slight decrease of the value of κ for the lighter Pt and the Os isotopes. The change in character of the spectra through both series of isotopes is essentially due to two effects: (i) the decrease of the value of χ_v, and (ii) the increase of the number of neutron bosons N_v. We note that the behaviour of ε, κ, χ_π and χ_v is in qualitative agreement with microscopic considerations [see eq. (3.1)]. It was found that both C_{0v} and C_{2v} vary from a repulsive value for $N \sim 118$ ($N_v = 4$) to an attractive value for $N \sim 108$ ($N_v = 9$). Such a behaviour agrees with the trend found in other regions [16]. The positive value of ξ_2 guarantees that no low-lying anti-symmetric multiplets occur for which there is no experimental evidence.

3.2. Pt ISOTOPES

The spectra and wave functions of those Pt isotopes for which $\chi_v \approx -\chi_\pi$ show many of the characteristics of the O(6) limit of the IBA-1 hamiltonian. Compared to the perturbed O(6) picture of IBA-1 [ref. [13]] the overall agreement with the experimental level scheme has improved: in contrast to IBA-1 the order of the 0_2^+ and 3_1^+ is correctly predicted in the heavier Pt isotopes and the position of the 2_3^+ state relative to the 0_2^+ state has also improved. We note that the position of the 3_1^+ state, although lower than in IBA-1, is still calculated too high, especially in ^{194}Pt. In the present case it would have been possible to further lower its energy by decreasing
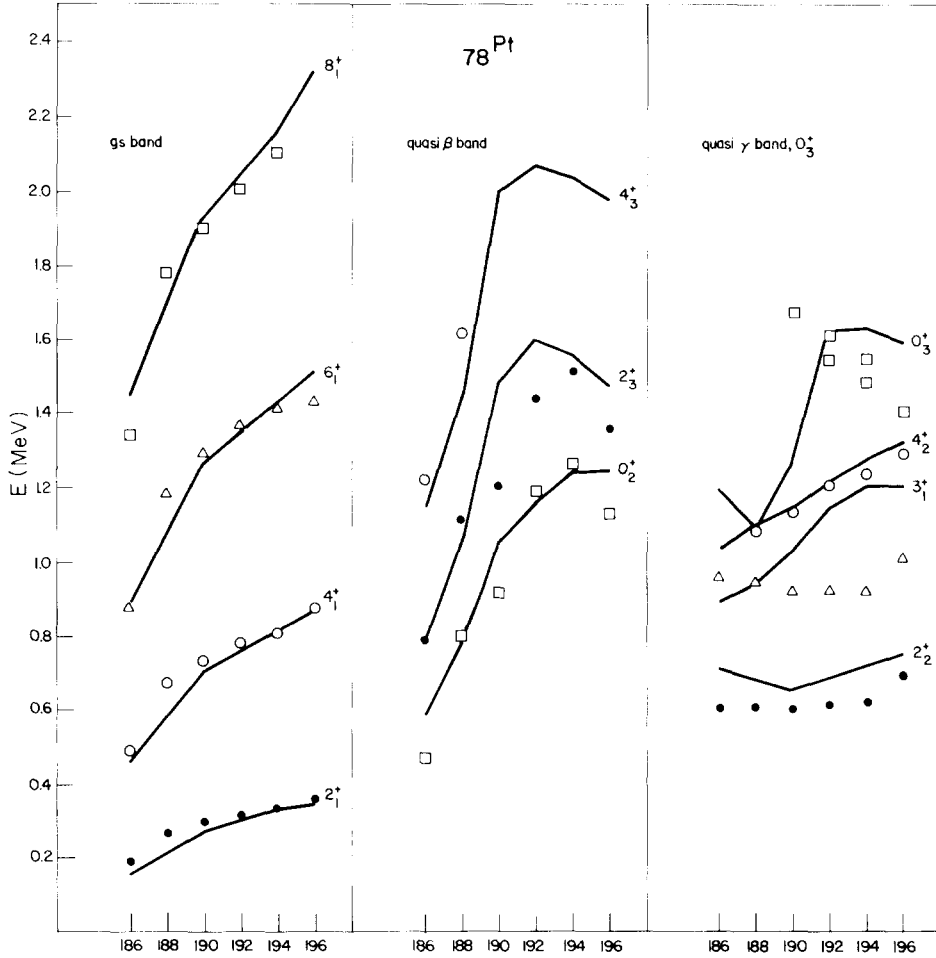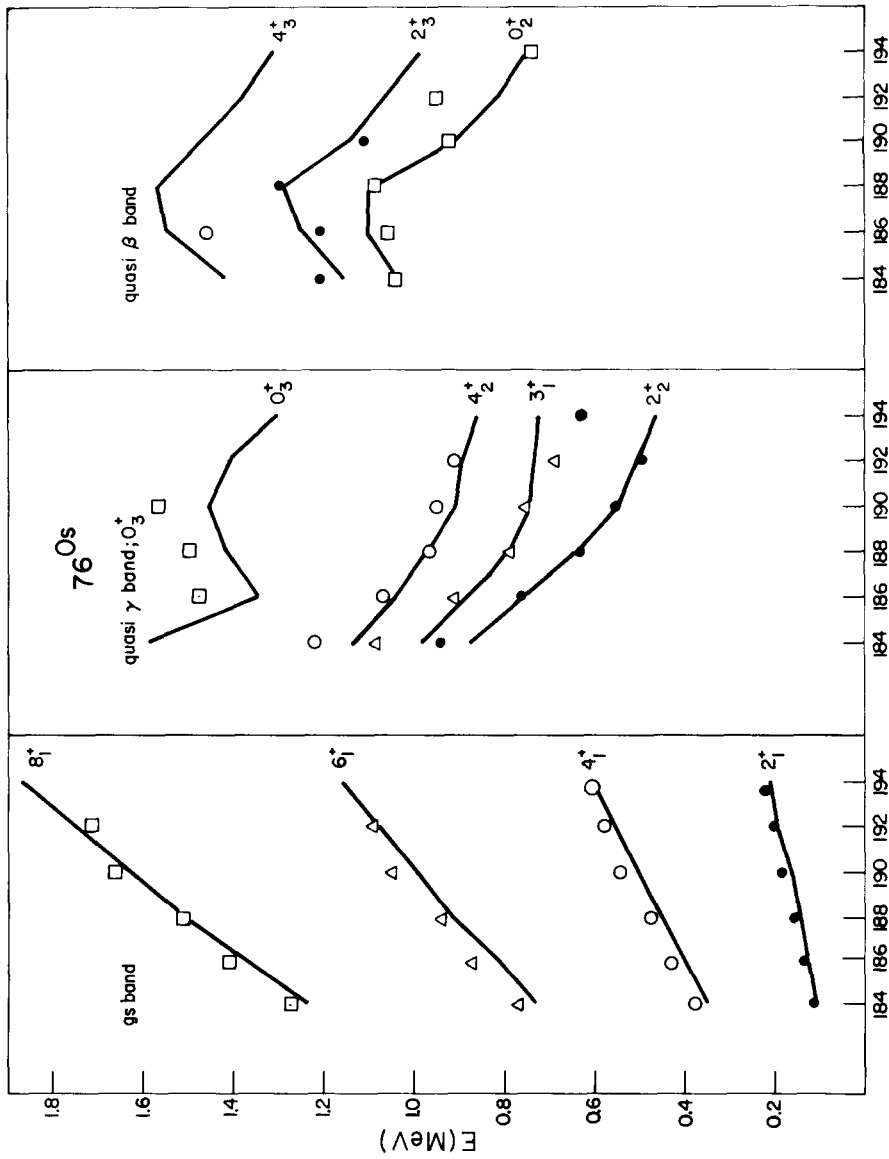
Fig. 1. Comparison between calculated and experimental energy levels in Pt. The experimental levels are taken from ref. [18].

the value of ξ_3. However, such a procedure seems rather *ad hoc* and has not been pursued. In the transitional region with increasing N_ν, the increase in the matrix elements of the $Q_\nu \cdot Q_\pi$ force (proportional to $N_\pi N_\nu$), in combination with an increase in $|\chi_\nu + \chi_\pi|$ gradually lead to a more SU(3) type spectrum [8]. The moment of inertia of the ground-state band increases, the quasi-γ band is pushed up, and the 0_2^+ becomes a member of a $K = 0$ β-band. It is seen that only one of the two 0^+ states observed around 1.5 MeV in ^{192,194}Pt is reproduced; one of these states probably does not have an SU(6) $\otimes$ SU(6) character.

Fig. 2. Comparison between calculated and experimental energy levels in Os. The experimental levels are taken from ref. [18].

3.3. THE Os ISOTOPES

The Os isotopes between mass number $A = 184$ and $A = 192$ exhibit a transition similar to the one between [186]Pt and [196]Pt. It is found that the Os and Pt isotopes can indeed be described with one set of parameters χ_ν (see table 1). With increasing boson number the moment of inertia of the ground-state band increases, the isotopes become more stable against γ-vibrations and the β-band shows a maximum excitation energy around $A = 188$. Here the character of the 0_2^+ state changes rather abruptly from a $\tau = 3$ state to a β-vibrational state. We note that the nucleus [194]Os forms an interesting puzzle. Two recent experiments [19]) have shown a rather large increase of the 2_2^+ energy with respect to [192]Os, even reversing the order of the 4_1^+ and the 2_2^+ states. In the present approach this effect cannot be reproduced, without substantial adjustment of the parameters χ_ν and χ_π.

The difference between the spectra for the Os and Pt isotopes can be ascribed to: (i) the larger value of $|\chi_\pi + \chi_\nu|$ for the Os isotopes and (ii) the larger proton boson number N_π in Os, which both lead to a stronger quadrupole-quadrupole interaction and thus to a spectrum with more SU(3) features.

3.4. TWO-NEUTRON SEPARATION ENERGIES

Within the framework of the present model we can also calculate binding energies. Returning to eq. (2.6) we note that for fixed proton-boson number N_π the two-neutron separation energies can be expressed as

$$S_{2\nu} = \mathrm{BE}(Z, N) - \mathrm{BE}(Z, N - 2) = E_0(N_\nu) - E_0(N_\nu + 1) + A'_\nu + B_\nu N_\nu, \qquad (3.2)$$

where $E_0(N_\nu)$ is the binding energy obtained with the hamiltonian (2.1) without the term H_C, and $A'_\nu = A_\nu + A_{\pi\nu} N_\pi$. The calculated separation energies are shown in fig. 3. The values of the parameters that are obtained from a fit to the data are $B_\nu = 0.609$ MeV, $A_\nu = 14.037$ MeV and $A_{\pi\nu} = -1.120$ MeV. It is seen that the effect of the change of character of the hamiltonian between the SU(3) and O(6) limits has only a minor effect on the slope of S_{2n}, this in contrast with the situation in the SU(5)–SU(3) transitional region [12]), where a clear signal of a shape phase transition is observed.

4. Electromagnetic transition rates

4.1. THE E2 OPERATOR

To the extent that the transition operator is a one-body boson operator the most general E2 operator can be expressed as

$$T(\mathrm{E2}) = e_\pi \bar{Q}_\pi^{(2)} + e_\nu \bar{Q}_\nu^{(2)}, \qquad (4.1)$$
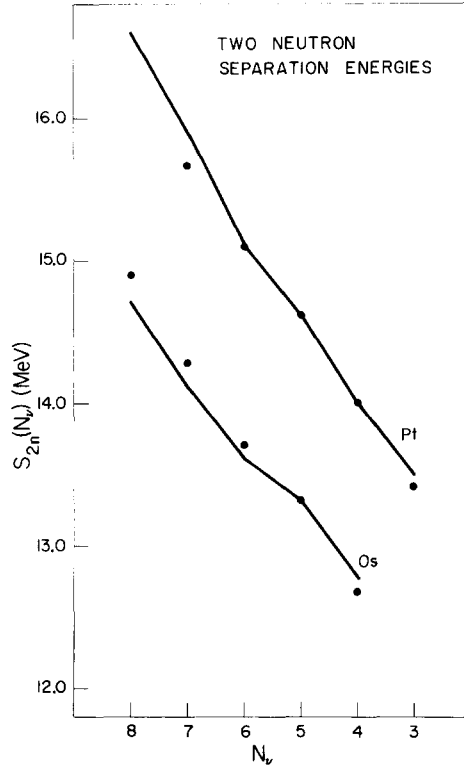
Fig. 3. Comparison between calculated and experimental two-neutron separation energies. The experimental values are taken from ref. [20].

where $\bar{Q}_\rho^{(2)} = (s_\rho^\dagger d_\rho + d_\rho^\dagger s_\rho)^{(2)} + \bar{\chi}_\rho (d_\rho^\dagger d_\rho)^{(2)}$, $\rho = \pi, \nu$. It seems natural to use in eq. (4.1) the same form for the neutron and proton quadrupole operators as in the hamiltonian (2.2), i.e. to set $\bar{\chi}_\pi = \chi_\pi$ and $\bar{\chi}_\nu = \chi_\nu$. The ratio of e_π and e_ν, required to fit experimental $B(E2)$ values, may depend on the precise nature of the experimental method used in determining E2 matrix elements, i.e. the extracted "$B(E2)$ value" may have different values for purely electromagnetic probes (Coulomb excitation, γ-decay, electron scattering) and for hadronic probes [(p, p'), (α, α'), $(\pi^\pm, \pi^\pm)$ reactions]. In fact one would expect that electromagnetic processes are relatively more sensitive to the proton distribution than hadronic processes, although it is well known that effects from core polarization tend to reduce the zeroth-order difference appreciably.

Due to lack of quantitative information in the following equal boson effective charges, $e_\pi = e_\nu$, will be used to describe the experimental $B(E2)$ values, unless stated otherwise.

Because of the large similarity of the structure of the quadrupole operator and the wave functions in the IBA-1 and IBA-2 approaches it is expected that the E2 selection rules in the present case are nearly the same as those in the IBA-1 model.
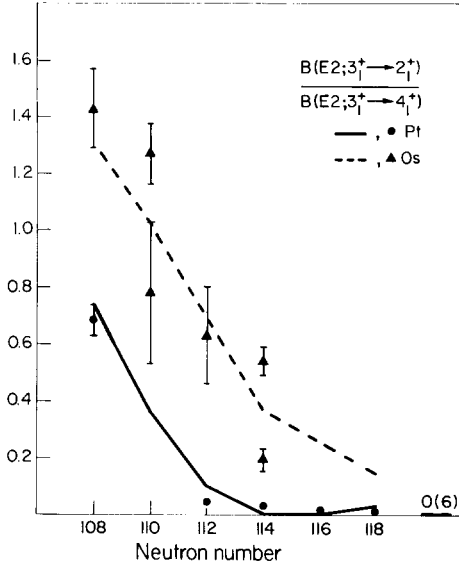
Fig. 4. Comparison between calculated and experimental values of the ratio $R_1 = B(E2; 3_1^+ \to 2_1^+)/B(E2; 3_1^+ \to 4_1^+)$. The experimental values are taken from refs. [21,25] (Pt) and refs. [22,27,30,35,38,39] (Os). In the SU(3) limit $R_1 = 2.50$. In the determination of the experimental $B(E2)$ values and branching ratios corrections for internal conversion have been taken into account; also corrections for M1/E2 mixing ratios have been included if these were known (figs. 4–11).
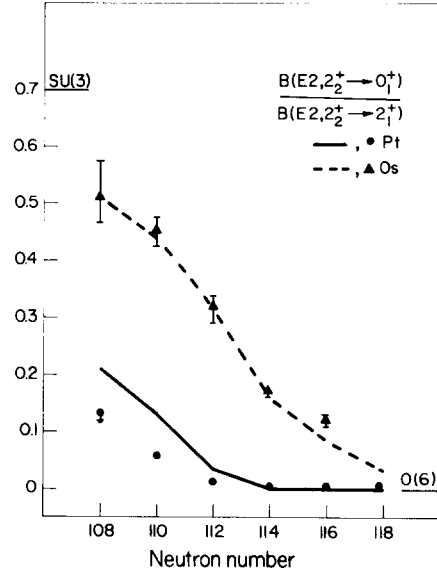
Fig. 5. Comparison between calculated and experimental values of the ratio $R_2 = B(E2; 2_2^+ \to 0_1^+)/B(E2; 2_2^+ \to 2_1^+)$. The experimental values are taken from refs. [21,25] (Pt) and refs. [27,28,30,32,33,35,39,40] (Os).

to the O(6) limit of IBA-1 where this transition is forbidden due to the $\Delta\sigma = 0$ selection rule). In the Os and the lighter Pt isotopes the 0_3^+ state has a different character and is expected to decay mainly to the 2_2^+ state (fig. 11).

It can be seen from the figures that in the O(6) region the weak transitions are also calculated to be weak, due to the $\Delta\tau = \pm 1$ selection rule. However, whereas some of the magnitudes of these transition ratios experimentally reach a minimum value in ^{196}Pt (for example, the ratios R_1, R_2 and R_6) the calculated position of the minimum (which in the present approach takes place when the neutron and proton contributions are equal in magnitude and opposite in sign) occurs in a lighter Pt isotope. The explanation is that the contribution to these ratios mainly comes from the d-boson conserving term; in the heavier Pt isotopes there is an effective breaking of the $\Delta\tau = \pm 1$ selection rule caused by the fact that $\chi_\nu \neq -\chi_\pi$.
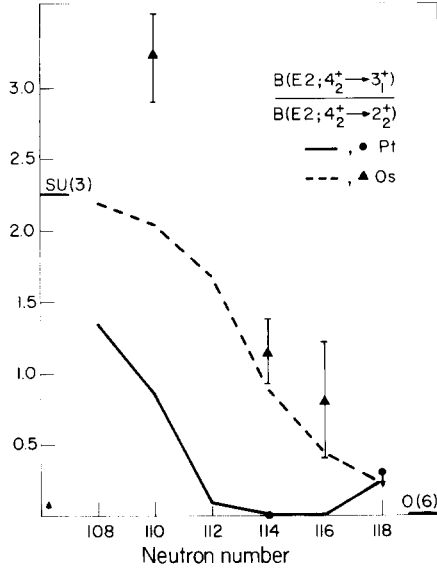
Fig. 6. Comparison between calculated and experimental values of the ratio $R_3 = B(E2; 4_2^+ \rightarrow 3_1^+)/B(E2; 4_2^+ \rightarrow 2_2^+)$. The experimental values are taken from ref. [13] (Pt), and refs. [30, 38-40] (Os).
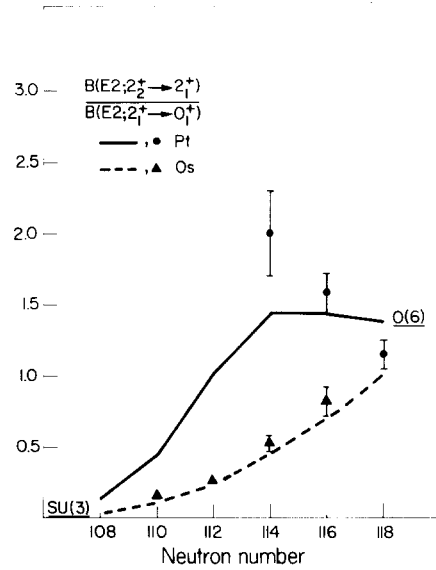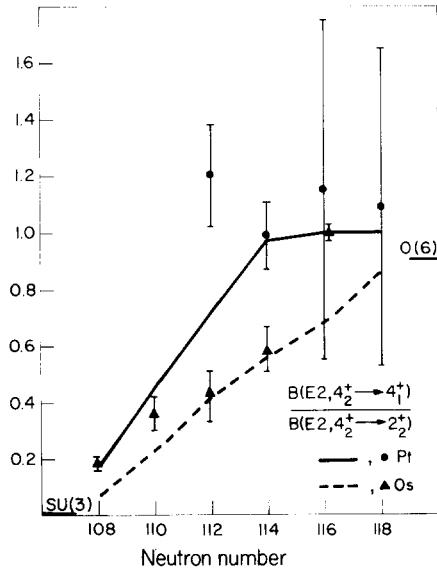
Fig. 7. Comparison between calculated and experimental values of the ratio $R_4 = B(E2; 2_2^+ \rightarrow 2_1^+)/B(E2; 2_1^+ \rightarrow 0_1^+)$. The experimental values are taken from refs. [23-25] (Pt) and refs. [32, 33] (Os).

Fig. 8. Comparison between calculated and experimental values of the ratio $R_5 = B(E2; 4_2^+ \rightarrow 4_1^+)/B(E2; 4_2^+ \rightarrow 2_2^+)$. The experimental values are taken from refs. [21, 22, 25, 45] (Pt) and refs. [22, 27, 30, 35, 38-41] (Os).
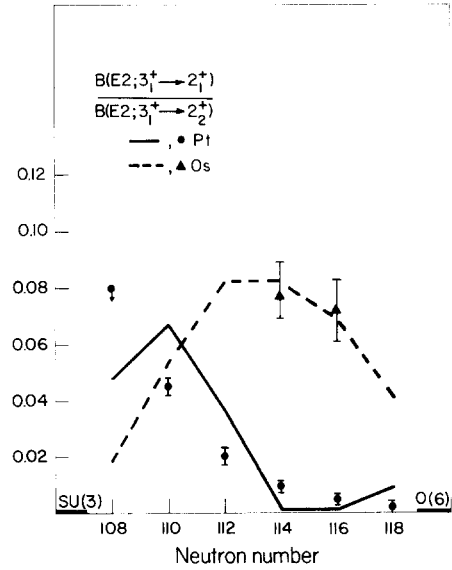
Fig. 9. Comparison between calculated and experimental values of the ratio $R_6 = B(E2; 3_1^+ \rightarrow 2_1^+)/B(E2; 3_1^+ \rightarrow 2_2^+)$. The experimental values are taken from refs. [21, 22, 26] (Pt) and refs. [38-40] (Os).
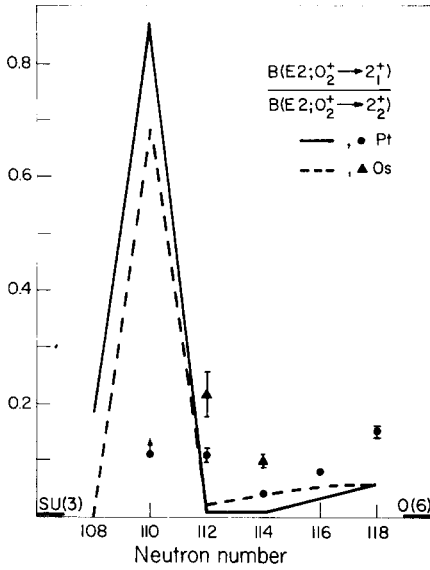
Fig. 10. Comparison between calculated and experimental values of the ratio $R_7 = B(E2; 0_2^+ \to 2_1^+)/B(E2; 0_2^+ \to 2_2^+)$. The experimental values are taken from refs. [21,26] (Pt) and refs. [35-38] (Os).
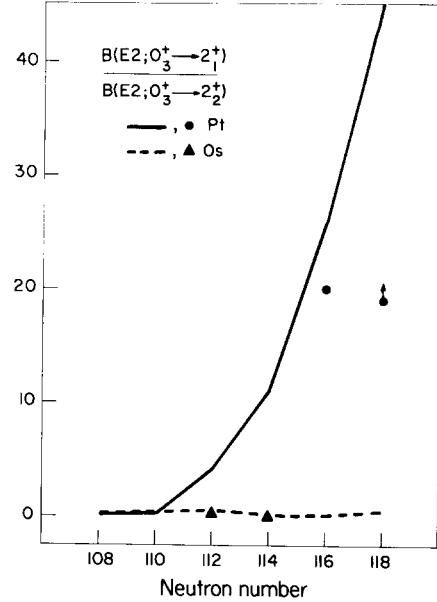
Fig. 11. Comparison between calculated and experimental values of the ratio $R_8 = B(E2; 0_3^+ \to 2_1^+)/B(E2; 0_3^+ \to 2_1^+)$. The experimental values are taken from ref. [26] (Pt) and refs. [35,37,38] (Os).

4.3. ABSOLUTE $B(E2)$ VALUES AND QUADRUPOLE MOMENTS

In calculating absolute $B(E2)$ values the simplest approach is to use boson effective charges $e_\nu = e_\pi = e_B$ which are constant for all nuclei. With the choice $e_B = 0.17 (e \cdot b)$ to fit the $B(E2; 2_1^+ \to 0_1^+)$ in ^{194}Pt we have calculated $B(E2)$ values in the nuclei ^{194,196}Pt, where there is much experimental information available. The results are listed in the tables 2 and 3 together with the results of IBA-1 [refs. [10,45]], those of Kumar and Baranger [5]) (KB) and those of Tamura and collaborators [3,34]). It is seen that whereas the O(6) limit of IBA-1 gives already a good description of the stronger E2 transitions the present calculation also accounts for the weak E2 transitions which correspond to a breaking of the O(6) selection rules. Furthermore the results of IBA-2 are very similar to those of the other calculations.

The following points are worth noting. First, all calculations overestimate the strength of the $0_2^+ \to 2_2^+$ transition in ^{196}Pt. Secondly, although the predicted quadrupole moments of the 2_1^+ states in IBA-2 have the correct sign they are too small. This discrepancy is very likely due to the fact that the value of $\chi_\pi + \chi_\nu$ for ^{194,196}Pt used in the present calculation (in which it has not been attempted to describe each nucleus in detail) is somewhat too small. Indeed we have checked that an increase of the value of $\chi_\pi + \chi_\nu$ in the hamiltonian (2.1) yields a larger value of $Q_{2_1^+}$ in these

TABLE 2

B(E2) values (in $e^2 \cdot b^2$) and quadrupole moment (in $e \cdot b$) for ^{196}Pt

Transition	Exp	IBA-2	IBA-1 [a]	WT [e]
$2_1^+ \to 0_1^+$	0.264 ± 0.011 [a] 0.309 ± 0.021 [b] 0.30 ± 0.02 [c]	0.289	0.264	0.273
$2_2^+ \to 2_1^+$	0.318 ± 0.023 [a] 0.342 ± 0.034 [b]	0.400	0.346	0.319
$2_2^+ \to 0_1^+$	3×10^{-6} [a]	9×10^{-7}	0	6×10^{-4}
$4_1^+ \to 2_1^+$	0.409 ± 0.022 [a]	0.395	0.346	0.433
$0_2^+ \to 2_2^+$	0.142 ± 0.077 [a]	0.465	0.352	0.388
$0_2^+ \to 2_1^+$	0.022 ± 0.010 [a]	0.025	0	0.048
$4_2^+ \to 4_1^+$	0.193 ± 0.097 [a]	0.206	0.167	0.183
$4_2^+ \to 2_2^+$	0.177 ± 0.025 [a]	0.205	0.184	0.248
$4_2^+ \to 2_1^+$	0.003 ± 0.001 [a]	0.005	0	0.0003
$6_1^+ \to 4_1^+$	0.421 ± 0.116 [a]	0.409	0.352	
$Q_{2_1^+}$	0.56 ± 0.21 [d] 0.49 ± 0.18 [d]	0.270	0	0.58

Parameters used in the calculation $e_\pi = e_\nu = e_B = 0.17 \, e \cdot b$.
[a] Ref. [45].   [b] Ref. [23].   [c] Ref. [21].   [d] Ref. [43].   [e] Ref. [34].

nuclei. Thirdly, the property of boson number conservation of the IBA model leads to a reduction of the intraband B(E2; $L+2 \to L$) values with increasing L compared to the predictions of other approaches. From fig. 12 one sees that the available experimental information does not allow one to draw definite conclusions about the presence of cut-off effects.

Finally we turn to a discussion of the trend of some E2 properties through the whole transitional region. In this case we compare two prescriptions for the choice of e_B: (i) assuming constant values of e_π and e_ν as above, and (ii) assuming that e_π and e_ν are equal in ^{194}Pt, but otherwise have the same dependence on $N_\nu(N_\pi)$ as $\kappa_\nu(\kappa_\pi)$ [see eq. (3.1)]. It is seen from fig. 13 that whereas with constant e_B the B(E2; $2_1^+ \to 0_1^+$) values increase too fast with increasing N_ν (curve A), with renormalized values of e_ν and e_π the observed values are very well reproduced (curve B). Also the trend of the weak B(E2, $2_2^+ \to 0_1^+$) (see fig. 14) and the quadrupole moments of the 2_1^+ states (see fig. 15) in the Os isotopes are very well described. As mentioned above the calculated values of $Q_{2_1^+}$ in the Pt isotopes appear to change sign too early.

4.4. THE SIGN OF P_4 IN ^{192,194}Pt

Recently it has been pointed out by several authors [46] that most collective models

TABLE 3

$B(E2)$ values (in $e^2 \cdot b^2$) and quadrupole moment (in $e \cdot b$) for ^{194}Pt

Transition	Exp	IBA-2	IBA-1 [f]	KT [d]	KB [e]
$2_1^+ \rightarrow 0_1^+$	0.374 ±0.016 [a] 0.324 ±0.003 [b]	0.357	0.37	0.318	0.341
$4_1^+ \rightarrow 2_1^+$	0.47 ±0.03 [a] 0.449 ±0.022 [b]	0.496	0.49	0.506	0.535
$6_1^+ \rightarrow 4_1^+$	0.32 ±0.08 [a] 0.48 ±0.14 [a]	0.544	0.52	0.626	
$8_1^+ \rightarrow 6_1^+$	0.36 ±0.11 [a]	0.515	0.48	0.713	
$4_2^+ \rightarrow 2_2^+$	0.28 ±0.12 [a] 0.18 ±0.06 [a] 0.69 ±0.39 [b]	0.275	0.27	0.302	
$6_2^+ \rightarrow 4_2^+$	0.28 ±0.06 [a]	0.318	0.33	0.468	
$8_2^+ \rightarrow 6_2^+$		0.272			
$2_2^+ \rightarrow 0_1^+$	0.0014±0.0002 [a] 0.0015±0.0002 [c]	3×10^{-5}	0	0.005	0.001
$2_2^+ \rightarrow 2_1^+$	0.58 ±0.07 [a] 0.423 ±0.015 [b] 0.60 ±0.07 [c]	0.517	0.49	0.351	0.451
$4_2^+ \rightarrow 4_1^+$	0.87 ±0.43 [b]	0.276		0.215	
$4_2^+ \rightarrow 2_1^+$	0.01 ±0.005 [b]	0.004		0.0003	
$Q_{2_1^+}$	0.63 ±0.06 [b] 0.62 ±0.18 [g]	0.13	0	0.68	0.49

Parameters used in the calculation $e_\pi = e_\nu = e_B = 0.17\,e \cdot b$.
[a] Ref. [24].   [b] Ref. [42].   [c] Ref. [23].   [d] Ref. [3].   [e] Ref. [5].   [f] Ref. [10].   [g] Ref. [43].

fail to predict the correct sign of P_4, a product of E2 matrix elements,

$$P_4 \doteq \langle 2_1^+\|T(E2)\|2_1^+\rangle\langle 0_1^+\|T(E2)\|2_1^+\rangle\langle 2_1^+\|T(E2)\|2_2^+\rangle\langle 0_1^+\|T(E2)\|2_2^+\rangle. \quad (4.2)$$

Experimentally, in ^{192,194}Pt one finds [46] $P_4 > 0$. It is obvious that the model dependence of the calculated sign of P_4 essentially arises from the very small matrix elements $\langle 0_1^+\|T(E2)\|2_2^+\rangle$. In fact in IBA-2 the smallness of this matrix element results from a delicate cancellation of neutron and proton boson contributions, and thus its sign sensitively depends on the actual values of e_ν and e_π. For ^{194}Pt the prescription $e_\nu/e_\pi = 1$ yields $P_4 < 0$; however, the observed sign of P_4 can be reproduced with a slightly different choice, for example $e_\nu/e_\pi = 1.2$. It is worth noting that such a change in e_ν/e_π would also improve the agreement with experiment of several other weak E2 matrix elements; for example, in ^{196}Pt the calculated values of $B(E2; 2_2^+ \rightarrow 0_1^+)$ and $R_6 = B(E2; 3_1^+ \rightarrow 2_1^+)/B(E2; 3_1^+ \rightarrow 2_2^+)$ are reduced considerably, improving the agreement with experiment. In ^{192}Pt a more complicated situation occurs. In the present calculation the value of the diagonal matrix element
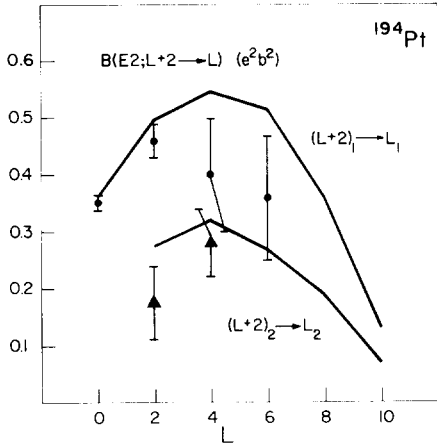
Fig. 12. Comparison between calculated and experimental $B(E2; L+2 \rightarrow L)$ values for ^{194}Pt. The experimental values are taken from refs. [24,42].
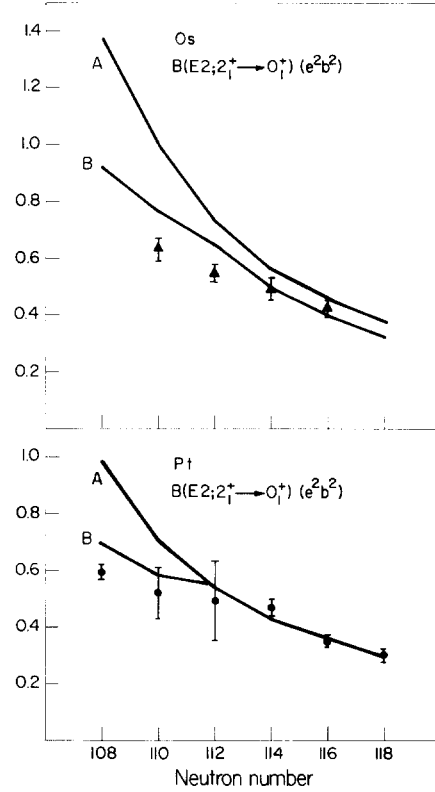
Fig. 13. Comparison between calculated and experimental values $B(E2; 2_1^+ \rightarrow 0_1^+)$ values. Curves A are calculated with constant boson effective charges whereas curves B are calculated with renormalized boson effective charges (see text). The experimental values are taken from refs. [21,23] (Pt) and refs. [32,33] (Os).

$\langle 2_1^+ \| T(E2) \| 2_1^+ \rangle$ is also very small (due to the fact that $\chi_\nu + \chi_\pi = 0$). Therefore the sign of P_4 is very sensitive to small variations of both e_ν / e_π and $\chi_\nu + \chi_\pi$, precluding a meaningful comparison with experiment.

5. Other observables

5.1. TWO-NUCLEON TRANSFER REACTIONS

In the framework of the IBA-2 the two-nucleon transfer intensities can easily be calculated. It has been shown [47]) that in lowest order the $L = 0$ two-neutron transfer operators $P_{\pm\nu}^{(0)}$ can be expressed as

$$P_{-\nu}^{(0)} = \alpha_\nu \sqrt{(\Omega_\nu - N_\nu)} s_\nu, \qquad P_{+\nu}^{(0)} = \alpha_\nu s_\nu^\dagger \sqrt{(\Omega_\nu - N_\nu)}, \tag{5.1}$$
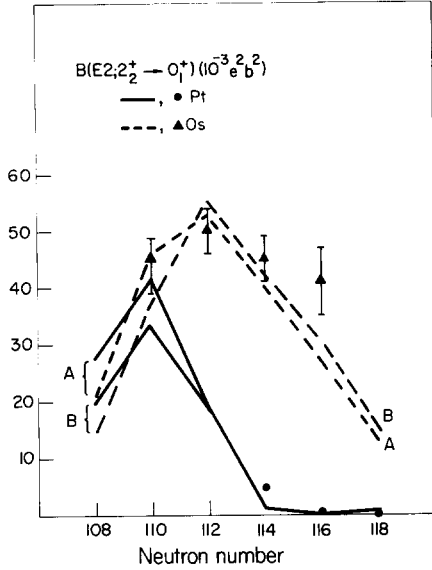
Fig. 14. Same as fig. 13 for the $B(E2; 2_2^+ \rightarrow 0_1^+)$ values. The experimental values are taken from refs. [23, 24]) for Pt and refs. [32, 33]) for Os.
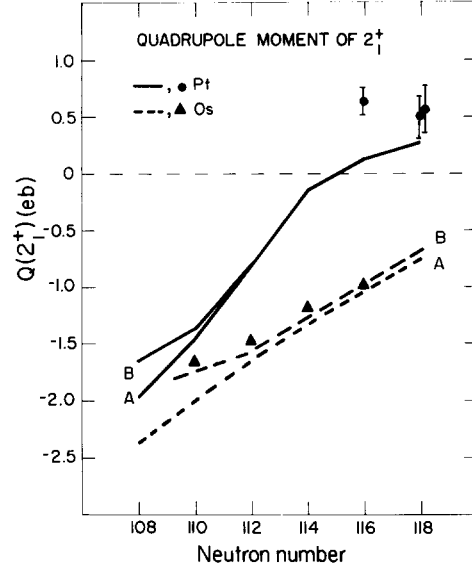
Fig. 15. Same as fig. 13 for the quadrupole moment of the 2_1^+ state, $Q_{2_1^+}$. The experimental values are taken from refs. [42, 43]) (Pt) and ref. [44]) (Os).

where α_v is a normalization constant. In the present case where the bosons are hole-like $P_{+v}^{(0)}$ describes the (p, t) reaction. The operator $s^\dagger$ has the following selection rules: in the O(6) limit $s^\dagger$ connects the $(\sigma = N, \tau = 0)$ ground state of the target nucleus with the $(\sigma = N+1, \tau = 0)$ ground state and the $(\sigma = N-1, \tau = 0)$ excited 0^+ state in the final nucleus; in the SU(3) limit $s^\dagger$ connects the $(\lambda, \mu) = (2N, 0)$ ground state of the target with the $(\lambda, \mu) = (2N+2, 0)$ ground state and the $(\lambda, \mu) = (2N-2, 2)$ excited 0^+ state in the final nucleus. On the other hand the operator s which enters in the $P_{-v}^{(0)}$ operator for the (t, p) reaction only connects ground states in both limiting cases.

Recent (p, t) experiments [48, 49]) on the Pt isotopes indicate a gradual change in the excitation pattern of the low-lying 0^+ states: in the heavy Pt isotopes the 0_2^+ state is excited with about 2 % of the ground-state strength and a higher-lying 0^+ is excited with about 5 % of the strength; on the other hand in ^{188}Pt the 0_2^+ state has 5 % of the strength and higher 0^+ states are not seen at all. It is seen in fig. 16 that the IBA calculation qualitatively agrees with the observed trend. We note that it is not always possible to uniquely associate a 0^+ IBA state with the observed higher 0^+ states. For example only one of two 0^+ states observed around 1.5 MeV excitation energy in ^{192,194}Pt is reproduced in our calculation. On the basis of the E2 decay properties it is tempting to associate the 0^+ state at 1480 keV in ^{194}Pt with the 0_3^+ state in IBA; however, in that case one cannot explain why this state is not seen in the (p, t) reaction.
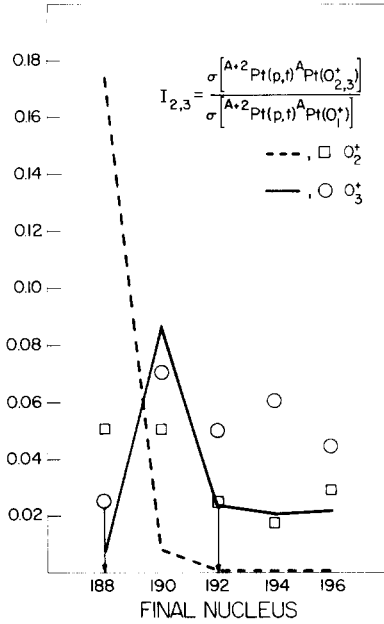
Fig. 16. Comparison between calculated and experimental Pt (p, t) transfer strengths relative to the ground-state strength. The experimental values are taken from refs. [48,49]. Uncertainties are (10–15)%.
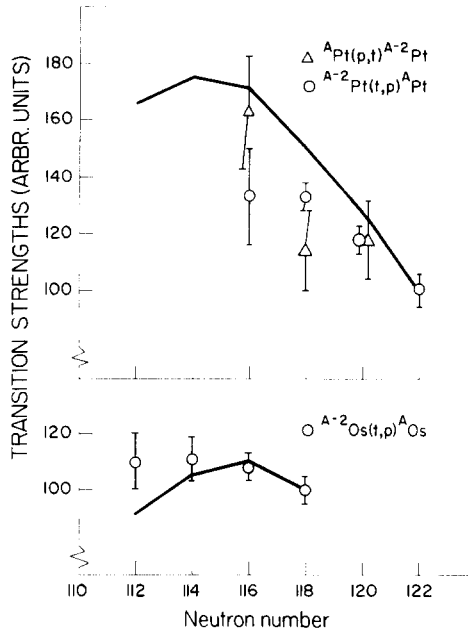
Fig. 17. Comparison between calculated and experimental (p, t) (triangles) and (t, p) (circles) ground-state transfer strengths, relative to the ^{198}Pt (t, p) empirical strength and to ^{192}Os (t, p). The experimental values are taken from ref. [50].

Also in a recent experiment the absolute (t, p) cross sections for the ground state transitions in the Os and Pt isotopes have been measured [50]. In fig. 17 the calculated and experimental transition strengths are compared.

5.2. E0 TRANSITIONS, ISOMER AND ISOTOPE SHIFTS

The most general one-body rank-zero operator can be written as

$$T^{(0)} = \beta_{0\pi}d_{\pi}^{\dagger} \cdot \tilde{d}_{\pi} + \beta_{0v}d_{v}^{\dagger} \cdot \tilde{d}_{v} + \gamma_{0\pi}N_{\pi} + \gamma_{0v}N_{v}. \qquad (5.2)$$

The following observables can be expressed in terms of the operator $T^{(0)}$:

(i) The isomer shift, which is the difference between the mean square radius $\langle r^2 \rangle$ of an excited state and the ground state in a given nucleus:

$$\delta\langle r^2 \rangle = \langle e|r^2|e \rangle - \langle 0|r^2|0 \rangle = \beta_{0\pi}\delta n_{d\pi} + \beta_{0v}\delta n_{dv}, \qquad (5.3)$$

where

$$\delta n_{d\rho} = \langle e|d_{\rho}^{\dagger} \cdot \tilde{d}_{\rho}|e \rangle - \langle 0|d_{\rho}^{\dagger} \cdot \tilde{d}_{\rho}|0 \rangle. \qquad (5.4)$$

(ii) The isotope shift, which is a measure of the difference in $\langle r^2 \rangle$ between two

neighbouring isotopes in their ground states:

$$\Delta\langle r^2\rangle = \langle 0|r^2|0\rangle_A - \langle 0|r^2|0\rangle_{A-2} = \beta_{0\pi}\Delta n_{d\pi} + \beta_{0\nu}\Delta n_{d\nu} - \gamma_{0\nu}, \qquad (5.5)$$

where

$$\Delta n_{d\rho} = \langle 0|d_\rho^\dagger \cdot \tilde{d}_\rho|0\rangle_{N_\nu} - \langle 0|d_\rho^\dagger \cdot \tilde{d}_\rho|0\rangle_{N_\nu+1}. \qquad (5.6)$$

(iii) The E0 transition matrix elements can be written as

$$\rho_{\mathrm{if}}(\mathrm{E0}) = \frac{Z}{R_0^2}\langle \mathrm{f}|r^2|\mathrm{i}\rangle = \frac{Z}{R_0^2}(\beta_{0\pi}\langle \mathrm{f}|d_\pi^\dagger \cdot \tilde{d}_\pi|\mathrm{i}\rangle + \beta_{0\nu}\langle \mathrm{f}|d_\nu^\dagger \cdot \tilde{d}_\nu|\mathrm{i}\rangle), \qquad (5.7)$$

where R_0 is the radius of the nucleus.

A striking feature of the observed isomer shifts is that in the Os isotopes the shifts for the 2_1^+ states are small and negative, and for the 2_2^+ states large and positive [ref. [51]]. This effect cannot be reproduced if only the proton contribution [$\beta_{0\nu} = 0$ in eq. (5.3)] is included. However, by allowing for independent effective contributions of neutrons and protons, $\beta_{0\pi} = -0.036$ fm^2 and $\beta_{0\nu} = 0.018$ fm^2, not only the isomer shifts in the Os isotopes can be reproduced but also those in the Pt isotopes (see table 4). With these values of $\beta_{0\pi}$ and $\beta_{0\nu}$ the isotope shift can be obtained by fitting the additional parameter $\gamma_{0\nu}$ [see eq. (5.5)]. In table 5 we compare the predicted isotope shifts ($\gamma_{0\nu} = -0.075$ fm^2) with those measured in the Os isotopes [52]. Finally the E0 transition matrix elements can be calculated without new free parameters. In table 6 we compare the calculated values of ρ(E0) with the available experimental information [53,54].

TABLE 4

Calculated and experimental isomer shifts

Nucleus	L^π	$\delta\langle r^2\rangle$ (10^{-3} fm^2)	
		exp	th
^{188}Os	2_1^+	−0.66	0.35
	2_2^+	16.5	15.93
^{190}Os	2_1^+	−1.73	−1.70
	2_2^+	17.2	15.47
^{192}Os	2_1^+	−2.33	−4.21
	2_2^+	9.1	11.62
^{194}Pt	2_1^+	3.45	3.62
	2_2^+	3.57	5.08
^{196}Pt	2_1^+	4.49	2.55

Parameters used in the calculation are:

$$\beta_{0\nu} = 18\times10^{-3}\ \mathrm{fm}^2,\ \beta_{0\pi} = -36\times10^{-3}\ \mathrm{fm}^2.$$

The experimental data are taken from ref. [51].

TABLE 5

Calculated and experimental isotope shifts in the Os isotopes

Isotope pair	$\Delta\langle r^2 \rangle$ (10^{-3} fm^2)	
	exp	th
$^{186-184}$Os	79 ± 17	54
$^{188-186}$Os	78 ± 16	56
$^{190-188}$Os	68 ± 14	70
$^{192-190}$Os	61 ± 12	77

ters used in the calculation are:

$$\beta_{0\nu} = 18 \times 10^{-3} \text{ fm}^2, \ \beta_{0\pi} = -36 \times 10^{-3} \text{ fm}^2, \ \gamma_{0\nu} = -75 \times 10^{-3} \text{ fm}^2.$$

The experimental data are taken from ref. [52].

6. Concluding remarks

In this paper we have described various properties of the Pt and Os isotopes in the framework of the IBA-2 model.

TABLE 6

E0 matrix elements

Nucleus	Transition	$\rho(E0)$	
		exp	th
^{188}Os	$0_2^+ \rightarrow 0_1^+$	2.2×10^{-2}	2.9×10^{-3}
	$2_2^+ \rightarrow 2_1^+$	$(2.2^{+0.8}_{-1.4}) \times 10^{-2}$	2.8×10^{-3}
^{190}Os	$2_2^+ \rightarrow 2_1^+$	$(2.5^{+1.5}_{-4.1}) \times 10^{-2}$	8.2×10^{-3}
		$-(7 \ \pm 15) \times 10^{-3}$	
^{192}Pt	$2_2^+ \rightarrow 2_1^+$	$(1.6 \pm 1.4) \times 10^{-2}$	1.0×10^{-2}
		$(1 \ ^{+20}_{-17}) \times 10^{-3}$	
		$(1.7 \pm 0.5) \times 10^{-2}$	
^{194}Pt	$2_2^+ \rightarrow 2_1^+$	$(10.9 \pm 6.6) \times 10^{-3}$	13.1×10^{-3}
^{196}Pt	$2_2^+ \rightarrow 2_1^+$	$(5.6 \pm 7) \times 10^{-2}$	1.5×10^{-2}
		$-(3.2 \pm 1.1) \times 10^{-2}$	
		$-(4 \ ^{+5}_{-4}) \times 10^{-3}$	
		$(1.6 \pm 0.2) \times 10^{-2}$	
		$(3.9 \pm 0.7) \times 10^{-2}$	

Parameters used in the calculation are:

$$\beta_{0\nu} = 18 \times 10^{-3} \text{ fm}^2, \ \beta_{0\pi} = -36 \times 10^{-3} \text{ fm}^2, \ R_0^2 = 50 \text{ fm}^2.$$

The experimental data are taken from refs. [53, 54].

The main part of the hamiltonian which determines the excitation energies of the low-lying states consists of two terms: (i) the single d-boson energy, ε, and (ii) the strength and shape of the quadrupole-quadrupole interaction between neutron and proton bosons (determined by the parameters κ, χ_ν and χ_π). Since in a isotopic chain χ_π is kept constant and the parameters ε and κ vary very little the characteristic changes in one series of isotopes are described mainly by the variation of only one parameter, χ_ν. (Vice versa in isotone direction, where χ_ν is constant, the trend can be reproduced by the variation of χ_π.) To obtain quantitative agreement with experiment it was found necessary to introduce also an interaction between neutron d-bosons.

One of the main advantages of the present approach over other calculations is its simplicity; although in the present investigation we have restricted ourselves to a description of nuclei with neutron number $N \geq 108$ the simple structure of the hamiltonian enables one to easily extend the calculations to nuclei further away from the closed shells. As an illustration we show in fig. 18 the predicted energy spectra of [168–196]Pt isotopes throughout the $N = 82$–126 neutron shell. The parameters used in calculating the lighter Pt isotopes were obtained from a simple extrapolation combined with some information obtained from fits to nuclei in the Sm, Gd region.

Finally we discuss some of the points on which the present results differ from the results of other calculations. First, compared to the calculation in the IBA-1
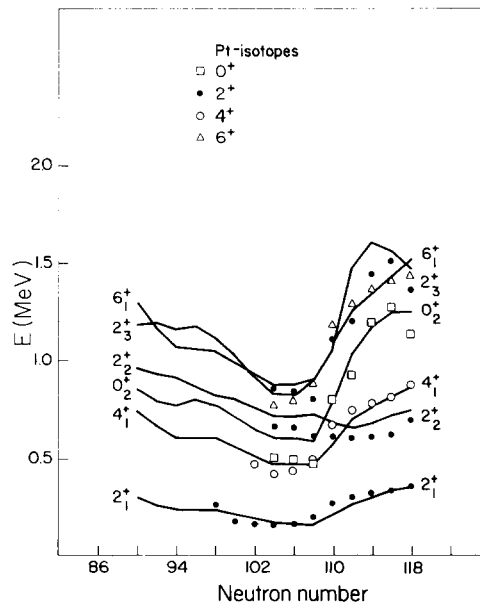

Fig. 18. Comparison between calculated and experimental energy levels in [168–196]Pt. The parameter set is given in table 7. The experimental values are taken from ref. [18].

TABLE 7

Extrapolated parameter set for Pt isotopes (in MeV)

Nucleus	ε	κ	χ_v	χ_π	C_{0v}	C_{2v}	C_{4v}	ξ_2	$\xi_1 = \xi_3$
^{184}Pt	0.58	−0.135	−0.30	−0.80	−0.25	−0.08	0.00	0.04	−0.10
^{182}Pt		−0.125	−0.20		−0.25	−0.04			
^{180}Pt		−0.115	−0.40		−0.20	−0.03			
^{178}Pt		−0.11	−0.50		−0.15	0.00			
^{176}Pt		−0.11	−0.50		−0.10	0.00			
^{174}Pt		−0.11	−0.80		0.00	0.00			
^{172}Pt		−0.11	−1.10		0.00	0.00			
^{170}Pt		−0.11	−1.10		0.00	0.00			
^{168}Pt		−0.11	−1.00		0.00	0.00			

approach it is found that (i) the energy levels agree better with experiment, especially in the O(6) limit; (ii) the excellent agreement between experimental E2 branching ratios and selection rules and the IBA-1 predictions persists also in IBA-2; (iii) the IBA-2 approach is capable of explaining the observed non-vanishing static quadrupole moments of the 2_1^+ states (although the calculated values in the Pt isotopes are too small). Turning to other systematic calculations in the same region [those of Kumar and Baranger [5]) in terms of the pairing model plus quadrupole model, and those of Tamura et al. [3,34]) using the boson expansion method] we find that all calculations have in common that the excitation energy of the 3_1^+ states (and to a lesser extent the 2_2^+ state) in the heavier Pt isotopes is predicted too high in comparison with experiment. Although in the present case this discrepancy is a factor of two smaller than in the other calculations it might suggest that degrees of freedom other than of the quadrupole type are present.

Concerning E2 branching ratios we find that in all calculations the overall trend is reproduced reasonably well; a noticeable difference is that in the present case the decay pattern of the 0_2^+ states in ^{192,194,196}Pt is described much better than in the calculation of ref. [5]). There is also a characteristic difference between the predictions of the various models that can be traced back to the requirement of boson number conservation in IBA, namely the occurrence of cut-off effects in B(E2) values with increasing angular momentum. More accurate experimental information is needed to test this prediction.

References

1) U. Mosel and W. Greiner, Z. Phys. **217** (1968) 256
2) R. Sedlmeyer, M. Sedlmeyer and W. Greiner, Nucl. Phys. **A232** (1974) 465
3) T. Kishimoto and T. Tamura, Nucl. Phys. **A270** (1976) 317
4) T. Tamura, K. Weeks and T. Kishimoto, Phys. Rev. **C20** (1979) 307
5) K. Kumar and M. Baranger, Nucl. Phys. **A122** (1968) 273
6) M. Baranger and K. Kumar, Nucl. Phys. **A110** (1968) 529; **A122** (1968) 241
7) A. Arima and F. Iachello, Ann. of Phys. **99** (1976) 253
8) A. Arima and F. Iachello, Ann. of Phys. **111** (1978) 201
9) A. Arima and F. Iachello, Phys. Rev. Lett. **40** (1978) 385
10) A. Arima and F. Iachello, Ann. of Phys. **123** (1979) 468
11) F. Iachello, ed., Interacting bosons in nuclear physics (Plenum, New York, 1979)
12) O. Scholten, F. Iachello and A. Arima, Ann. of Phys. **115** (1978) 325
13) R. F. Casten and J. A. Cizewski, Nucl. Phys. **A309** (1978) 477
14) A. Arima, T. Otsuka, F. Iachello and I. Talmi, Phys. Lett. **66B** (1977) 205;
    T. Otsuka, A. Arima, F. Iachello and I. Talmi, Phys. Lett. **76B** (1978) 139
15) T. Otsuka, A. Arima and F. Iachello, Nucl. Phys. **A309** (1978) 1
16) F. Iachello, G. Puddu, O. Scholten, A. Arima and T. Otsuka, Phys. Lett. **89B** (1979) 1;
    G. Puddu, O. Scholten and T. Otsuka, Nucl. Phys. A, to be published
17) T. Otsuka, thesis, University of Tokyo
18) M. Sakai and Y. Gono, Quasi-ground, quasi-beta and quasi-gamma bands, Preprint INS-J-160 (1979)
19) R. F. Casten, A. I. Namenson, W. F. Davidson, D. D. Warner and H. G. Börner, Phys. Lett. **76B** (1978) 280;
    E. R. Flynn and D. G. Burke, Phys. Rev. **C17** (1978) 501
20) A. H. Wapstra and K. Bos, Atomic Data and Nucl. Data Tables **19** (1977) 175
21) M. Finger, R. Foucher, J. P. Husson, J. Jastrzebski, A. Johnson, G. Astner, B. R. Erdal, A. Kjelberg, P. Patzelt, A. Hoglund, G. Malmskog and R. Henck, Nucl. Phys. **A188** (1972) 369
22) S. W. Yates, J. C. Cunnane, R. Hochel and P. J. Daly, Nucl. Phys. **A222** (1974) 301
23) I. Berkes, R. Rougny, M. Meyer-Levy, R. Chéry, J. Danière, G. Lhersonneau and A. Troncy, Phys. Rev. **C6** (1972) 1098
24) K. Stelzer, F. Rauch, Th. W. Elze, Ch. E. Gould, J. Idzko, G. E. Mitchell, H. P. Nottrodt, R. Zoller, H. Wollersheim and H. Emling, Phys. Lett. **70B** (1977) 297
25) J. A. Cizewski, R. F. Casten, G. J. Smith, M. L. Stelts, W. R. Kane, H. G. Börner and W. F. Davidson, Phys. Rev. Lett. **40** (1978) 167
26) J. A. Cizewski, R. F. Casten, G. J. Smith, M. R. Macphail, M. L. Stelts, W. R. Kane, H. G. Börner and W. F. Davidson, Nucl. Phys. **A323** (1979) 349
27) R. Hochel, P. J. Daly and K. J. Hofstetter, Nucl. Phys. **A211** (1973) 165
28) T. Yamazaki, K. Nishiyama and D. L. Hendrie, Nucl. Phys. **A209** (1973) 153
29) R. Spanhoff, H. Postma and M. J. Canty, Phys. Rev. **C18** (1978) 493
30) B. Fogelberg, Nucl. Phys. **A197** (1972) 497
31) K. J. Hofstetter, T. T. Sugihara and D. S. Brenner, Phys. Rev. **C8** (1973) 2442
32) R. F. Casten, J. S. Greenberg, S. H. Sie, G. A. Burginyon and D. A. Bromley, Phys. Rev. **187** (1969) 1532
33) W. T. Milner, F. K. McGowan, R. L. Robinson, P. H. Stelson and R. O. Sayer, Nucl. Phys. **A177** (1971) 1
34) K. J. Weeks and T. Tamura, Phys. Rev. Lett. **44** (1980) 533
35) R. Thompson, A. Ikeda, R. K. Sheline, J. C. Cunnane, S. W. Yates and P. J. Daly, Nucl. Phys. **A245** (1975) 444
36) M. R. Macphail, R. F. Casten and W. R. Kane, Phys. Lett. **59B** (1975) 435
37) M. D. Svoren, E. F. Zganjar and I. L. Hawk, Z. Phys. **A272** (1975) 213
38) R. F. Casten, M. R. Macphail, W. R. Kane, D. Breitig, K. Schreckenbach and J. A. Cizewski, Nucl. Phys. **A316** (1979) 61
39) S. W. Yates, J. C. Cunnane, P. J. Daly, R. Thompson and R. K. Sheline, Nucl. Phys. **A222** (1974) 276

40) R. F. Casten, H. G. Börner, J. A. Pinston and W. F. Davidson, Nucl. Phys. **A309** (1978) 206
41) R. J. Gehrke, Nucl. Phys. **A204** (1973) 26
42) C. Baktash, J. X. Saladin, J. J. O'Brien and J. G. Alessi, Phys. Rev. **C18** (1978) 131
43) J. E. Glenn and J. X. Saladin, Phys. Rev. Lett. **20** (1968) 1298
44) M. V. Hoehn, E. B. Shera, Y. Yamazaki and R. M. Steffen, Phys. Rev. Lett. **39** (1977) 1313
45) R. F. Casten, private communication to F. Iachello
46) L. Hasselgren, C. Fahlander, J. E. Thun, A. Bockisch and F. J. Bergmeister, Phys. Lett. **83B** (1979) 169;
    F. T. Baker, Phys. Rev. Lett. **43** (1979) 195
47) A. Arima and F. Iachello, Phys. Rev. **C16** (1977) 2085
48) M. Vergnes, G. Rotbard, J. Kalifa, J. Vernotte, G. Berrier, R. Seltz and H. L. Sharma, Bull. Am. Phys. Soc. **21** (1976) 976
49) P. T. Deason, C. H. King, T. L. Khoo, J. A. Nolen and F. M. Bernthal, to be published
50) J. A. Cizewski, E. R. Flynn, R. E. Brown and J. W. Sunier, Phys. Lett. **88B** (1979) 207
51) R. Engfer, H. Schneuwly, J. L. Vuilleumier, H. K. Walter and A. Zehnder, Nucl. Data Tables **14** (1974) 509
52) K. Heilig and A. Stendel, Nucl. Data Tables **14** (1974) 613
53) A. V. Aldushchenkov and N. A. Voinova, Nucl. Data Tables **11** (1972) 299
54) B. L. Birbrair, N. A. Voinova and N. S. Smirnova, Nucl. Phys. **A251** (1975) 169